Atmospheric Environment 103 (2015) 129–137

Contents lists available at ScienceDirect

Atmospheric Environment

journal homepage: www.elsevier.com/locate/atmosenv

Seasonal variation of CO_2 diffusion flux from a large subtropical reservoir in East China

Fushun Wang [a, *], Man Cao [a], Baoli Wang [b], Jianan Fu [a], Wenyun Luo [a], Jing Ma [a]

[a] School of Environmental and Chemical Engineering, Shanghai University, Shanghai, 200444, China
[b] State Key Laboratory of Environmental Geochemistry, Institute of Geochemistry, Chinese Academy of Sciences, Guiyang, 550002, China

HIGHLIGHTS

- We report the CO_2 emission from a subtropical large reservoir.
- Reservoir surface can absorb large amount of atmospheric CO_2 in warm seasons.
- Downstream the dam has the similar contribution of CO_2 emission to reservoir surface.

ARTICLE INFO

Article history:
Received 9 April 2014
Received in revised form
1 December 2014
Accepted 17 December 2014
Available online 18 December 2014

Keywords:
CO_2 diffusion flux
Seasonal patterns
Subtropical reservoir
The Xinanjiang Reservoir

ABSTRACT

The Xinanjiang Reservoir (E118°42′–E118°59′, N29°28′–N29°58′), has a surface area of 567 km^2, with a mean water depth of 34 m, and is in an oligotrophic state at present. In this study, five cruises were carried out in April, June, August and November 2010, and January 2011, to understand the seasonal variation of CO_2 emission and to estimate the annual diffusion flux of CO_2 from this reservoir. The partial pressure of CO_2 (pCO_2) in surface water was determined using a continuous measurement system (equilibrator-infrared system) from upstream to central reservoir, and pCO_2 along the water column in central reservoir and in downstream of the dam was also determined. Results showed that pCO_2 in reservoir surface water varied significantly in different seasons, ranging from 5 μatm in August to 1700 μatm in January; while in downstream of the dam, it ranged from 1400 μatm in April to 3800 μatm in August. Along the water column in central reservoir, pCO_2 also showed significantly variations seasonally, and a water mass with quite high pCO_2 (>4000 μatm) formed below water depth of 20 m in warm seasons. The highest diffusion flux of CO_2 ($F–CO_2$) appeared in January, with values of 20.9 mmol m^{-2} d^{-1} at river reach and 25.2 mmol m^{-2} d^{-1} at central reservoir, while the lowest values of $F–CO_2$ were −10.0 at river reach and −10.8 mmol m^{-2} d^{-1} at central reservoir in August. Downstream of the dam had quite high positive $F–CO_2$ during the whole year, with a range of 129.1 in April to 381.5 mmol m^{-2} d^{-1} in August. In total, about 88.9 kton a^{-1} CO_2 was emitted to the atmosphere from the Xinanjiang Reservoir surface, while 39% of it (35.1 kton a^{-1}) was absorbed by surface water in warm seasons. Downstream and turbine had a comparable CO_2 outgas flux of 61.5 kton a^{-1}. When taking the whole reservoir surface, turbine and downstream into account, the Xinanjiang Reservoir system had a net CO_2 emission flux of 115.3 kton a^{-1}.

1. Introduction

Currently, carbon dioxide (CO_2) emission accounts for the largest share of greenhouse gases (GHGs) equivalent of 80–85% of the emissions (Tremblay et al., 2005). Since the industrial revolution, atmospheric CO_2 concentration has increased from 280 ppm to 389.85 ppm in 2010 (http://www.esrl.noaa.gov). Among the major anthropogenic sources of CO_2, fossil fuel burning has always been considered as the highest contributing factor. In order to alleviate the CO_2 emissions, clean energy development and utilization, especially hydropower exploitation, have been vigorously promoted (Chamberland and Levesque, 1996; Victor, 1998). As a result, large numbers of artificial hydropower reservoirs have been

* Corresponding author. School of Environmental and Chemical Engineering, Shanghai University, P.O. Box 144, 99 Shangda Road, Baoshan, Shanghai, 200444, China.
E-mail address: fswang@shu.edu.cn (F. Wang).

http://dx.doi.org/10.1016/j.atmosenv.2014.12.042
1352-2310/

constructed worldwide, with the estimation that "some 40,000 large dams (defined as more than 15 m in height) and more than 800,000 smaller ones are in operation, and more are still being constructed" (Humborg et al., 2002), and references therein.

However, recent researches showed that artificial reservoirs might also be a potential CO_2 contributors to the atmosphere (Kelly et al., 1997; Duchemin et al., 1995; St Louis et al., 2000; Fearnside, 2002; Dos Santos et al., 2006; Huttunen et al., 2002; Teodoru et al., 2012; Raymond et al., 2013) and have called the green credentials of hydropower into question (Giles, 2006). For example, some hydroelectric reservoirs in tropical regions were reported emitting more CO_2 per unit generating capacity than thermal power did (Dos Santos et al., 2006; Fearnside, 2002). The decomposition of flooded biomass and autogenetic organic matter is the major mechanism that produces GHG, which is composed of CO_2 and CH_4. Thus, the quantity of organic matter and the depositional environment in the reservoirs become determining factors for the production of GHG. In boreal and tropical reservoirs, flooded area generally has a higher density of soil organic carbon (OC), which will gradually be mineralized to CO_2 or CH_4 under oxygen-deficient condition after impounding. In addition, submerged vegetative cover in tropical area also provides abundant biomass to sedimentary OC in reservoir. These factors together made reservoirs in boreal and tropical area become the hotspots for GHG emission research (Abril et al., 2005; Demarty et al., 2009; Roland et al., 2010).

Nevertheless, little research has been devoted to the GHG emission from subtropical reservoirs. In fact, large numbers of reservoirs are operating in subtropical areas. Such as, over 40,000 reservoirs have been constructed in the Yangtze River basin, which is the longest river in Asia and the third-longest in the world. Furthermore, the characteristics of the reservoirs, including capacity, retention time, and the geological background, are diverse in different climate regions, which might induce different GHG emission flux. Consequently, it is potentially inaccurate to apply a uniform model to extrapolate the global reservoir GHG emission from different types of reservoirs. Therefore, investigating representative reservoirs in different climate areas is crucial to the estimation of the global GHG emission from reservoirs. In this study, the Xinanjiang Reservoir, a large subtropical reservoir, was investigated through five cruises carried out from 2010 to 2011. The main objectives were to understand the seasonal patterns of the pCO_2 in the Xinanjiang Reservoir, and to estimate the annual CO_2 diffusion flux contribution to the atmosphere. Moreover, the impact of deep-water discharge from the hydropower reservoir on the downstream CO_2 emission was also discussed in this study.

2. Study area and methodology

The Xinanjiang River is the mainstream of the Qiantang River, the largest river in Zhejiang Provence, East China, and has a length of 589 km and drains an area of 55,600 km^2. The Xinanjiang Reservoir (E118°42′–E118°59′, N29°28′–N29°58′), located in the Chun'an County, Zhejiang Province, was constructed in 1959, also known as the Qiandao Lake. It has a surface area of 567 km^2, with the mean and maximum water depths of 34 m and 117 m, respectively. The climate is typically subtropical monsoon climate with air temperature ranging from −5 °C to 36 °C (annual average value of 17 °C) and the annual precipitation of 1429.9 mm on average. The air humidity here is about 76% and forest coverage rate of the drainage area reaches 83%.

Cruise route began from the upstream (site A) to middle reach (site B), and finished at the central reservoir (site C) (Fig. 1). Five cruises were carried out during April, June, August and November 2010, and January 2011. In each cruise, surface water (0.3 m below water surface) was pumped (by a self-priming pump. Model: IZDB-

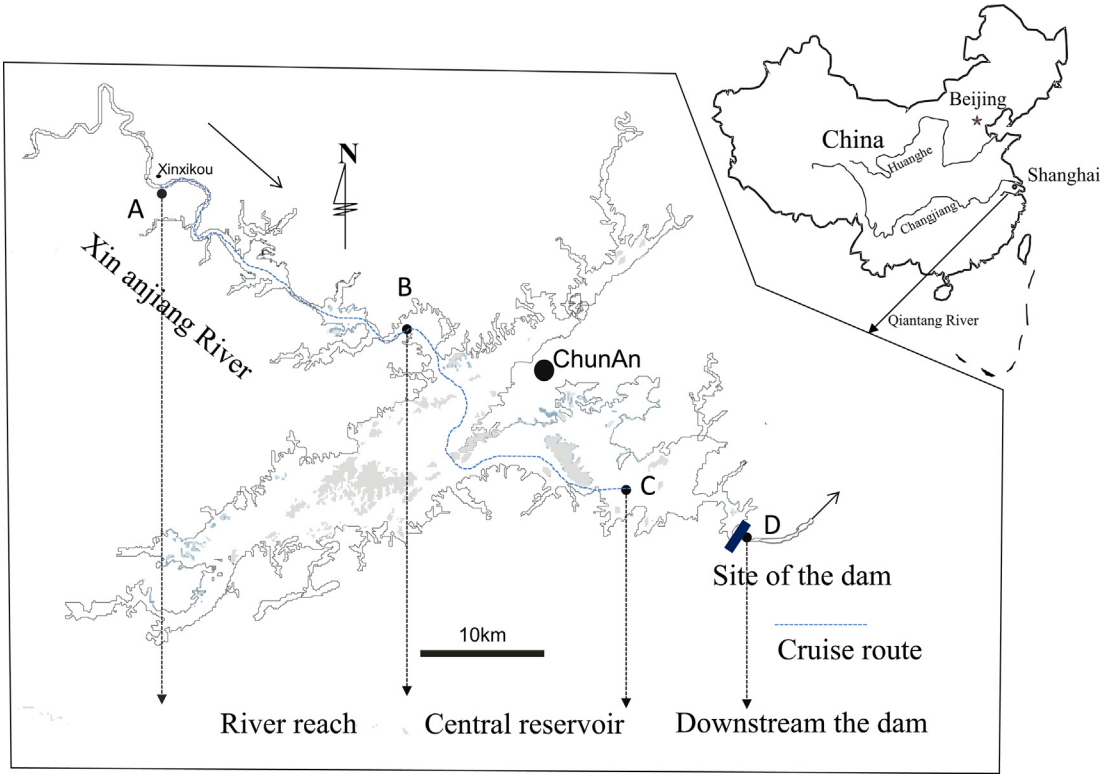

Fig. 1. Geographic location of the study area and the sampling sites.

35; Max. Flow: 40 L/min; Manufacturer: Yixing Co.) into a small barrel to continuously measure temperature, *p*H, and dissolved oxygen (DO) using an YSI-6600v2 meter. At the same time, pumped surface water was introduced into a continuous flow equilibrator to determine pCO_2 using a CO_2 non-dispersive infrared analyzer (Model: CA-10a, Sable Systems Co.), which has an accuracy of 1% of reading typical over range of 0–5% CO_2, with the resolution up to 0.0001% (1 ppm), and it also measure the pressure inside the analyzer cell with a resolution of 0.001 kPa. Signal drift of this analyzer is less than 0.001%/h.

The whole cycle of equilibrator is composed of an equilibrator and external facilities (including air pump, drying pipe, airflow control unit, and a CO_2 analyzer). The equilibrator is similar to the one of Frankignoulle et al. (2001) with a few differences. It combines a showerhead and a plexiglas cylinder (diameter 10 cm, height 40 cm) which is filled with glass marbles. Water was continuously pumped into the equilibrator at a speed of 3 L min^{-1} from the top shower head. For CO_2 determination, headspace air was introduced into a carbon dioxide analyzer (CA-10a) by an air pump at a speed of 1 L min^{-1}, after passing through a drying pipe (magnesium perchlorate) equipped to remove water vapor. We used equation (1) to express pCO_2 in 100% humidity (Copin-Montegut, 1985).

$$pCO_2 = pCO_2' \times (p - f)/(p + \Delta p) \quad (1)$$

where pCO_2' refers to the partial pressure of CO_2 in dry air. p is the pressure in inside the analyzer cell, which is regarded as the pressure in equilibrator due to the low flow rate of the air pump. Δp is the pressure difference between equilibrator and atmosphere, and was neglected for the reason that the equilibrator is open to atmosphere by a 5 m thin pipe. f is the partial pressure of water vapor at the temperature of the measurement.

Before the start of each cruise, carbon dioxide analyzer was calibrated by different gas standard with CO_2 concentrations ranging from 0, 300, 500, 1600, 2900, 3500 to 5000 ppm.

Along the water column in central reservoir, a diving pump (Model: 100QJ2-50/10; Flow rate: 2 m^3/h; Shanghai Xinlian Pump Valve Co.) was lowered down to pump deep water on board with the sampling interval of 5 m. The same procedure to cruise monitoring (equilibrator – non-dispersive infrared CO_2 analyzer system and YSI) was used to determine pCO_2 and in situ parameters. pCO_2 in downstream of the Xinanjiang dam was also determined. During the cruise, the sampling route was recorded by GPS, in order to match the monitoring data with the sampling position. Wind speed was measured by a portable anemometer when the cruise stopped.

The diffusion flux of CO_2 between water–air interface can be calculated with the Equation (2):

$$F = k(pCO_{2w} - gas_{sat})K_H \quad (2)$$

where, F is the diffusion flux of CO_2 between water and the atmosphere; pCO_{2w} is the partial pressure of CO_2 in the surface water; and gas_{sat} is the partial pressure of CO_2 in the water equilibrated with the overlying atmosphere CO_2 (385 μatm, at the sampling year 2010). K_H is Henry's constant, computed from temperature. The piston velocity, k (cm h^{-1}), of CO_2 at the water–air interface, can be affected by different factors such as current, turbidity, and wind speed (Abril et al., 2000). Considering the relatively low flow speed (<0.1 m s^{-1}) in central reservoir and its river reach, the following equations were used to calculate the k (Cole and Caraco, 1998; and references therein).

$$k = k_{600}(Sc/600)^{-0.67} \quad (3)$$

$$Sc(CO_2) = 1911.1 - 118.11t + 3.4527t^2 - 0.04132t^3 \quad (4)$$

$$k_{600} = 2.07 + 0.215U_{10}^{1.7} \quad (5)$$

$$U_{10} = 1.22U_1 \quad (6)$$

where, $Sc(CO_2)$ is the Schmidt number for CO_2, and k_{600} is the gas exchange coefficient normalized for CO_2 at 20 °C in fresh water with Schmidt number 600. U_1 is the wind speed at water surface, and U_{10} is the wind speed at 10 m above water surface. Wind speed in the studied area varied from 0 to 2.5 m s^{-1}, with an annual average value of 2.1 m s^{-1}. Under some extreme cases, wind speed can reach to more than 5 m s^{-1}, but this weather condition rarely appeared during the whole year. So, it was excluded from this calculation. Equations (3)–(6) are not appropriate for the estimation of k in downstream the dam, due to its high flow speed (ca. 1.0 m s^{-1}). Here, we estimated a k of 10 cm h^{-1}, by comparing its hydrographic features with other reported rivers (Aucour et al., 1999; Yang et al., 1996; Yao et al., 2007; Wang et al., 2011).

3. Results

3.1. Longitudinal variations in the surface water and vertical variation along the water column of water temperature and DO

Water temperature in the reservoir surface water ranged from 11 °C in winter to 35 °C in summer (Fig. 2a), showing an increasing pattern from upstream to central reservoir, except in April when rainy season was started. Water temperature in the downstream of the dam dropped sharply, with a narrower range of 11–15.5 °C. An obvious temperature discontinuity was developed up and down the dam. For instance, in August, the difference in temperature between the reservoir surface and downstream reached to 20 °C.

Fig. 3a showed the developing process of thermal stratification along the water column of the Xinanjiang Reservoir. A steady water layer with relative high temperature was formed in the epilimnion in warm seasons, which prevented the vertical mixing of water. As a result, the temperature differences between the epilimnion and 30 m below surface were up to 14.4 °C in June and 22.3 °C in August. This process also restricted the exchange of dissolved substances in the upper and lower layer. When water temperature decreased in winter, thermal stratification disappeared, and as a result, chemical stratification (such as, pCO_2, and DO, see below) also faded away.

Dissolved oxygen (DO) is an important indicator of photosynthesis and respiration in the water. DO will be over-saturated when primary production is prevailing in the water, and under-saturated when respiration is dominating. Our results showed that the saturation degrees of DO in the surface water of the reservoir were around 90–95% in November and January, accompanied by relative higher pCO_2, which indicated the influence of respiration in water (Fig. 2b). On the contrary, DO was obviously over-saturated during warm seasons, revealing the dominating of photosynthesis in the surface water. From upstream to central reservoir, DO showed a less longitudinal variation, but a more obvious seasonal variation. Throughout the whole year, DO in the downstream of the dam was under-saturated, with a range of 60–86%, suggesting the potential influence of deep-water discharge for hydropower generation.

Vertically, DO had an obvious seasonal distribution along the water column (Fig. 3b). Starting from April, a water mass with DO oversaturated was gradually formed above 5 m in depth, while

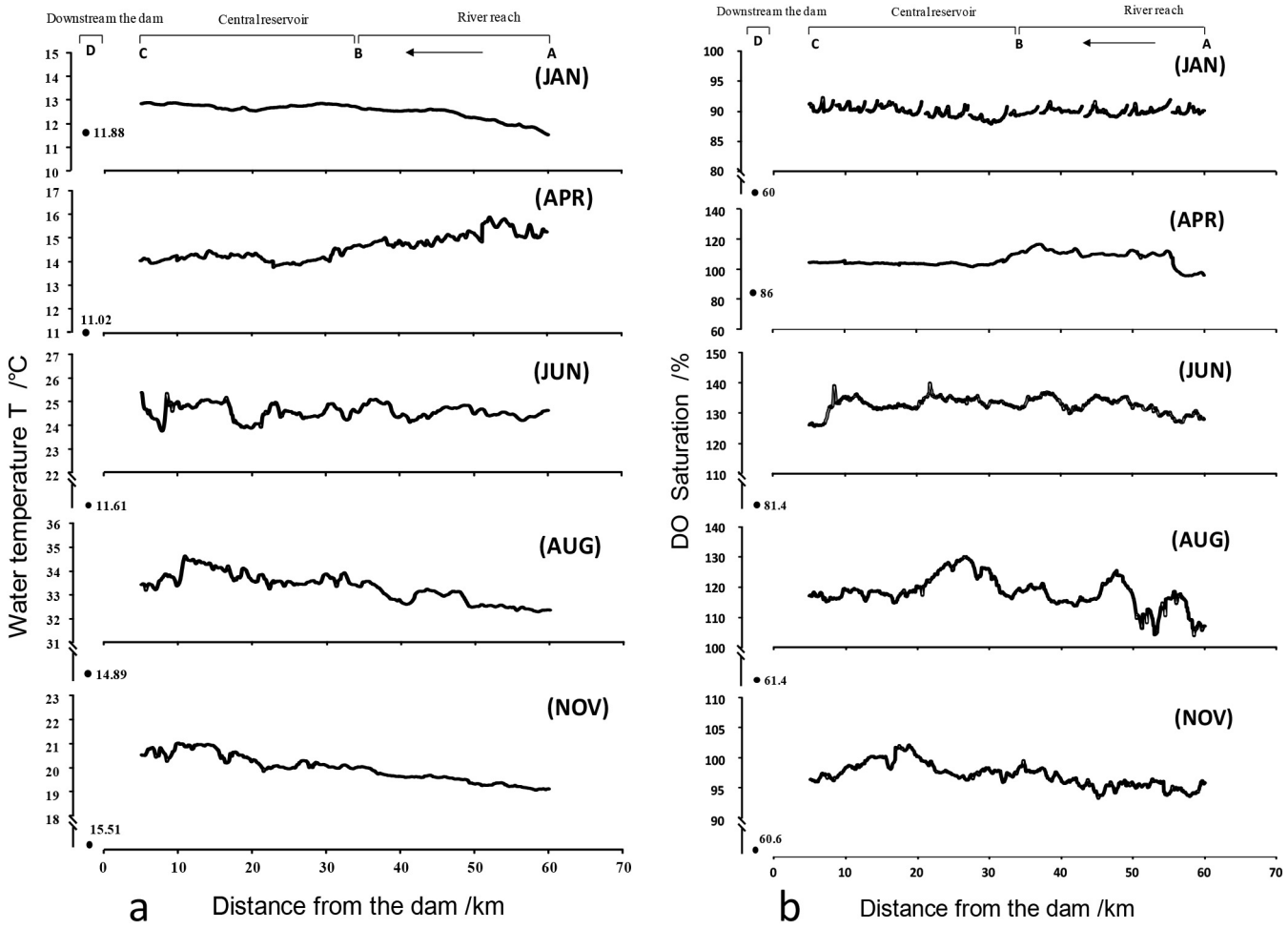

Fig. 2. Longitudinal variations of water temperature (a) and DO (b) in the surface water along the Xinanjiang Reservoir.

water below 20 m in depth became oxygen-deficit. This vertical DO structure was maintained till the end of October. With the collapse of thermal stratification in cold seasons, water was well mixed along the water column and the difference of DO was disappeared as well.

3.2. Longitudinal and vertical variation of pCO_2 and pH

The net gradient between pCO_2 in the surface water of the reservoir and the atmospheric CO_2 (385 μatm) was expressed as ΔpCO_2, whose seasonal and spatial patterns are shown in Fig. 4. The ΔpCO_2 varied significantly in different seasons, revealing a picture of under-saturation or oversaturation of CO_2 to atmosphere CO_2. Fig. 4 outlined two basic patterns of ΔpCO_2. In cold seasons (November and January), ΔpCO_2 varied from 323 to 1337 μatm. On the contrary, ΔpCO_2 became negative values with a range from −384 to −275 μatm in warm seasons (June and August). The values of ΔpCO_2 in the downstream of the dam were significantly higher than those in the surface of the reservoir in all seasons. The annual average value in the downstream of the dam was 2130 μatm, with a range of 1000–3420 μatm.

Similar to that in the surface water, pCO_2 in central reservoir also showed significant seasonal, as well as vertical variations along the water column (Fig. 3c). Although there was no obvious change of pCO_2 along the water column in January, the stratification of pCO_2 along the water column gradually developed with increasing ambient temperature. Especially, markedly CO_2 under-saturation occurred in water above 5 m in depth in June and August, characterized by pCO_2 obviously lower than the atmospheric level, which corresponded to the stratification of DO (Fig. 3b), indicating the prevailing of primary production in the epilimnion. However, during the same period, a water mass with quite high pCO_2 (>4000 μatm) formed below water depth of 20 m. This could explain the observed high values of pCO_2 in the downstream (Fig. 4), due to the deep water discharge from this reservoir.

pH values were detected ranging from 6.7 to 9.2 in the surface water of the reservoir during the whole year. Generally, in warm seasons (June and August), pH of the surface water in reservoir was above 8.5, with an average of 8.9. CO_2 showed extreme deficit in water under this pH. In contrast, pH in cold seasons was relative lower than that in warm seasons. From November to January, surface water in across the reservoir to the upstream had a stable pH, with a narrow scope of 7.35–7.6 (see Supplementary material for cruise monitor data, Dataset S1). pH in downstream of the dam was obviously lower than that in the reservoir surface water in all seasons, with an annual average of 6.91.

3.3. Diffusion of CO_2

Average values of pCO_2 in river reach and central reservoir of each cruise were used to calculate the diffusion of CO_2 at water–air interface, and the results were shown in Fig. 5. At river reach and

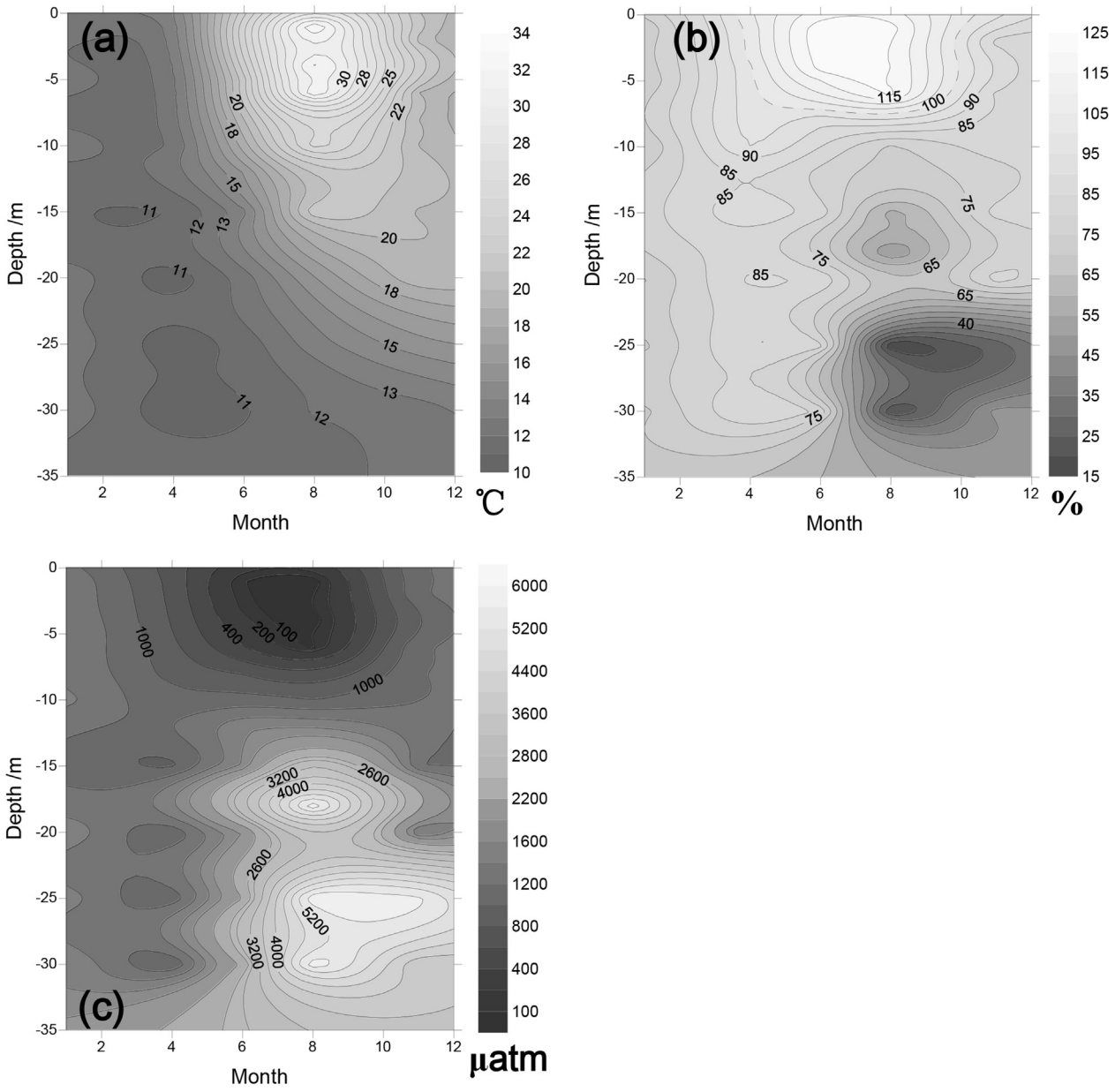

Fig. 3. Contours of water temperature (a), DO (b), and pCO_2 (c) along the water column in the central reservoir.

central reservoir, F—CO_2 varied significantly in different seasons. The lowest F—CO_2 appeared in August with values of −10.0 mmol m^{-2} d^{-1} at the river reach and −10.8 mmol m^{-2} d^{-1} at the central reservoir, respectively, indicating an important invasion of atmospheric CO_2. In cold seasons, the whole reservoir surface had positive values of F—CO_2, which reached the highest values of 20.9 mmol m^{-2} d^{-1} at river reach and 25.2 mmol m^{-2} d^{-1} at central reservoir in January respectively. These results suggest that the reservoir surface can play different roles as source or sink to atmospheric CO_2 in different seasons. The reservoir emits CO_2 to atmosphere in cold seasons, and absorbs CO_2 from atmosphere in warm seasons. However, in comparison to the reservoir surface, downstream of the dam had quite high positive F—CO_2 throughout the whole year, with a range of 129.1 in April to 381.5 mmol m^{-2} d^{-1} in August. This implies that deep-water discharge is potentially the important CO_2 emission channel from the reservoir.

4. Discussion

The mineralization of organic carbon to CO_2 significantly affects the pCO_2 in flowing water, and most rivers consequently maintain pCO_2 levels supersaturated with respect to the atmosphere (Richey, 2003; Barth et al., 2003; Cole and Caraco, 2001; Hélie et al., 2002; Richey et al., 2002; Jarvic et al., 1997; Raymond et al., 1997). In some specific cases, geogenic origin input of DIC from deep geothermal springs also can sustain the super-saturation of CO_2 in lake water (Borges et al., 2014). When the natural river was converted into artificial reservoir, seasonal thermal stratification will generally develop along the water column, which is mainly controlled by the water retention time. This may induce the prevailing of photosynthesis in epilimnion, together with the decrease of turbidity and flow speed. As a result, pCO_2 in water will be drawn down, due to the enhancement of photosynthesis. Under the condition of algae bloom, dissolved CO_2 could become obviously

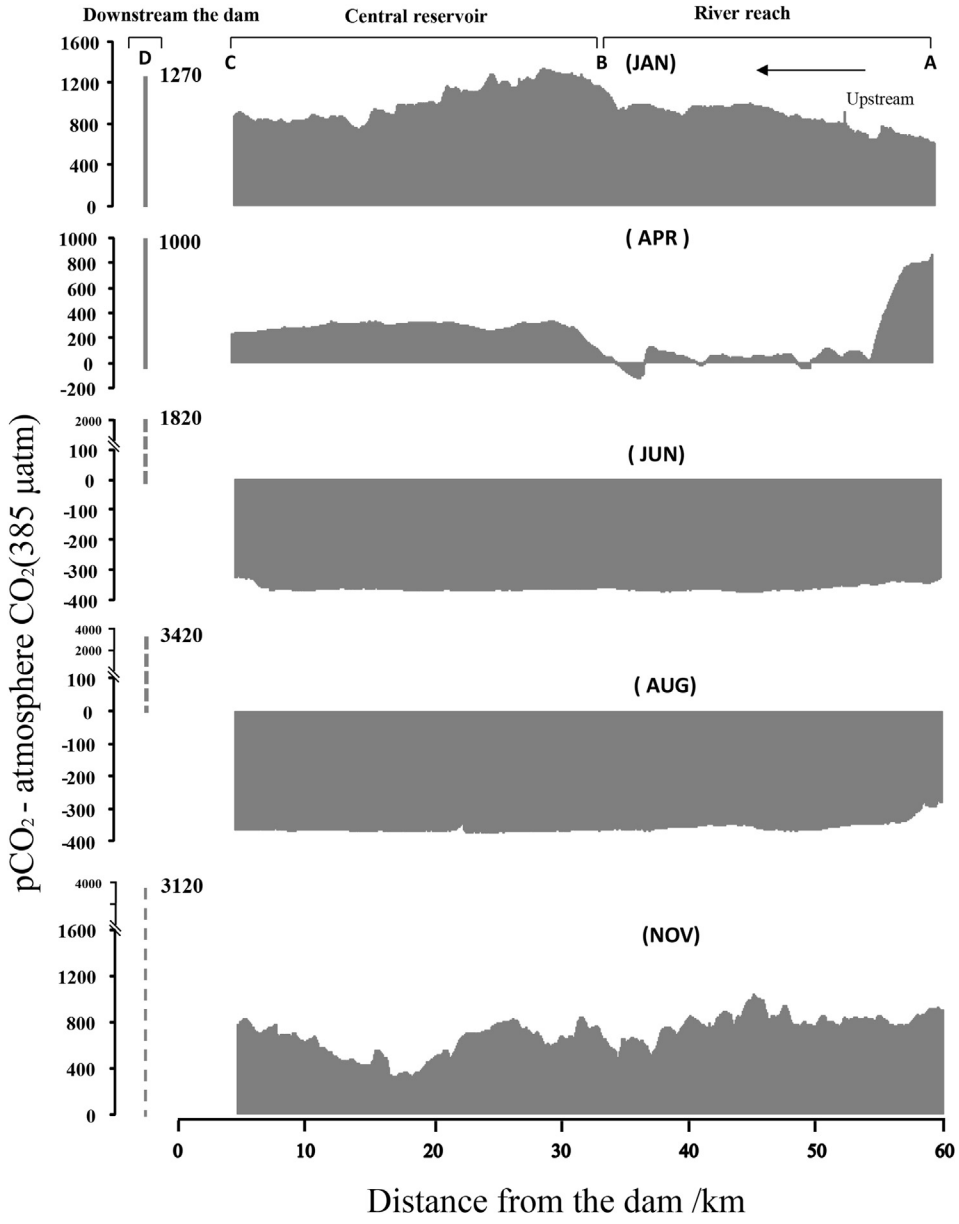

Fig. 4. The variation of the net values between pCO_2 in the surface water and the atmospheric CO_2 along the Xinanjiang Reservoir.

deficit, with pCO_2 lower than the atmosphere level but the supersaturation of DO, such as in June and August (Figs. 2 and 4). On the contrary, deep waters have higher pCO_2, but generally with a lower pH and DO, due to the respiration process dominated in the hypolimnion, specifically during the period of thermal stratification (Fig. 3). This shift between photosynthesis and respiration along water column in the central reservoir is clearly showed by the negative correlation between DO and pCO_2 (Fig. 6). Consequently, deep water in the reservoir generally had higher pCO_2 and lower DO and pH than surface water. Extremely, a water mass with quite high pCO_2 can persist in deep water, due to the thermal stratification in warm seasons, which is also shown in Fig. 3. Considering the deep water discharge for hydropower generation, downstream of the dam will consequently have high pCO_2, and significant CO_2 emission hence can occur (i.e. Figs. 4 and 5).

Recent study showed that newly constructed reservoir had quite high spatial heterogeneity of surface CO_2 fluxes (Roland et al., 2010; Teodoru et al., 2011). Comparatively, the Xinanjiang Reservoir had less variation of CO_2 flux from river reach to central reservoir (Fig. 5). The major reason is that the Xinanjiang Reservoir was constructed 60 years ago, and impounded landscape hence contributed less CO_2 to water. Barros et al. (2011) also reported an age model of CO_2 flux from global reservoirs. Our results basically is essentially compatible to this model, but whether the results fit their latitude model is uncertain, due to the empty data around 30° of latitude in their model. However, besides the age of reservoir, the retention time may be another important factor that impacts CO_2 flux from reservoir surface. Fig. 7a shows an exponential decline of CO_2 emission flux with the increase of retention time of the reservoirs within latitude between 18° and 47° ($r^2 = 0.32$; $n = 31$; $p < 0.001$). When only include reservoirs in the latitude between 20° and 30°, regression model fits the data better ($r^2 = 0.46$; $n = 20$; $p = 0.001$) (Fig. 7b). This indicates that, hydrological retention time has a severe influence on the CO_2 emission flux from the reservoir in low to mid-latitude areas. In general, after early decomposition and CO_2 releasing of the impounded vegetation cover, DOC and POC

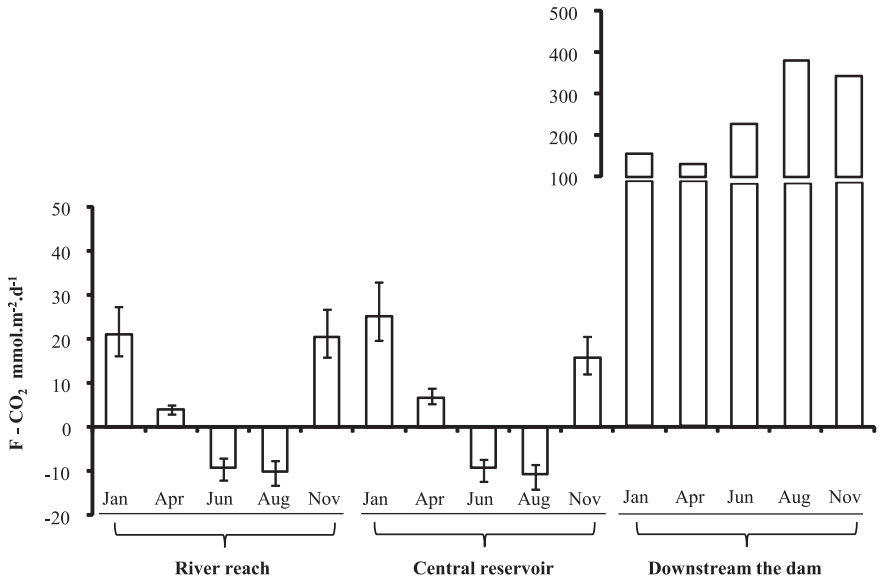

Fig. 5. Diffusion flux of CO_2 from the river reach, central reservoir and downstream the dam of the Xinanjiang reservoir (Data were calculated at wind speed of 1.5 m s^{-1}. Error bars were the results at wind speed 0 m s^{-1} and 2.5 m s^{-1} respectively).

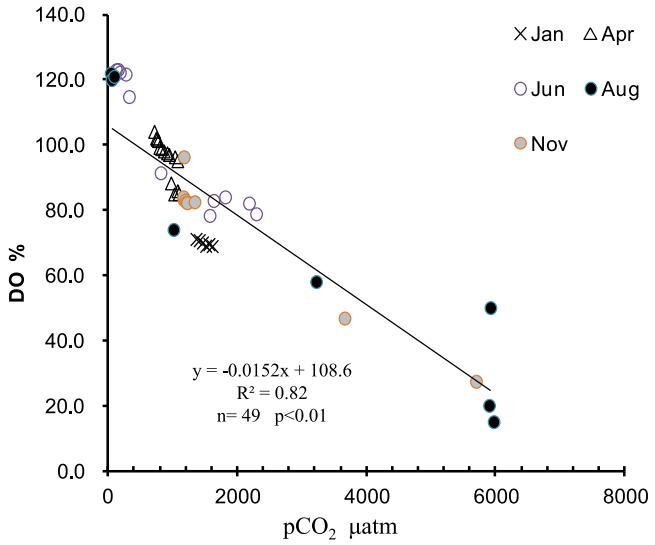

Fig. 6. Plot of DO versus pCO_2 along the water column in the central Xinanjiang Reservoir.

from the drainage basin become the major sources of CO_2 emitted from reservoir. In reservoirs with short retention time, it may keep the characteristics of river to some extent. For example, the mainstream of the Three Gorge Reservoir (with a retention time around 35 days), still keep one dimensional flow regime for the whole year, and thus has a high CO_2 emission flux (Xiao et al., 2013). Fig. 7 show that reservoirs with retention time less than around 60 days have the obviously higher flux.

However, in reservoirs with long retention time, POC is more easily deposited in sediment, and thus can avoid decomposition. On the other side, nutrients input and the development of thermal stratification also favors the increase in primary production, which is responsible for the sequestration of CO_2. Consequently, CO_2 emission fluxes from the reservoirs decreased exponentially with the increase of retention time, and gradually approaching a similar level of natural lakes (St Louis et al., 2000). It should be mentioned that, data from reservoirs in high latitude and tropical area was not included in this retention time model (Fig. 7), due to the possibility of ice coverage and melting in high latitude reservoirs. Reservoirs in tropical area generally have quite high CO_2 emission, which should be explained by other mechanisms.

Based on the results of CO_2 diffusion flux (Fig. 5), the annual CO_2 emission from reservoir surface was evaluated, as listed in Table 1. Due to difficulty of obtaining the surface area of downstream and the uncertainty of the anthropogenic perturbation, such as nutrients input, aquiculture, which will significantly change pCO_2, we assumed that pCO_2 in the downstream of the dam decreased to atmospheric CO_2 level and this difference was used to calculate the CO_2 emission. This method may bring an overestimation of CO_2 emission from the downstream, since CO_2 in river water generally is not always equilibrated to atmospheric CO_2, before it reaches to ocean. Totally, about 88.9 kton a^{-1} CO_2 was emitted to the atmosphere from the Xinanjiang Reservoir surface, while 39% of it (35.1 kton a^{-1}) was re-absorbed by surface water in warm seasons. As a result, annually the net emission flux of CO_2 from reservoir surface was about 53.8 kton. Despite its small water area, downstream had a comparable CO_2 outgas flux of 52.3 kton a^{-1}, which could be revealed by the quite high CO_2 diffusion flux at downstream (Fig. 5). Turbine degassing contributed 9.2 kton CO_2 a^{-1} to the atmosphere. When taking the whole reservoir surface, turbine and downstream into account, the Xinanjiang Reservoir system had a net CO_2 emission flux of 115.3 kton a^{-1}.

Compared with other reservoirs in different climate regions (see Supplementary material Table S1), the Xinanjiang Reservoir had obviously lower CO_2 diffusion flux, with a value of 5.3 ± 14.5 mmol m^{-2} d^{-1} from the reservoir surface. This flux is lower than that from temperate reservoirs and natural lakes, and is at the similar level with that of some boreal reservoirs. However, downstream the dam of the Xinanjiang Reservoir had significantly high CO_2 emission flux, and hence became an important channel for CO_2 emission, from which about 52.3 kton CO_2 a^{-1} was emitted. Tropical reservoirs generally had quite high CO_2 emission fluxes not only from the reservoir surface, but downstream of the dam. For instance, despite one third less in reservoir surface area than the Xinanjiang Reservoir, the Petit Saut had a total emission of 309.1 kton CO_2 a^{-1}, which is twice the flux of the Xinanjiang.

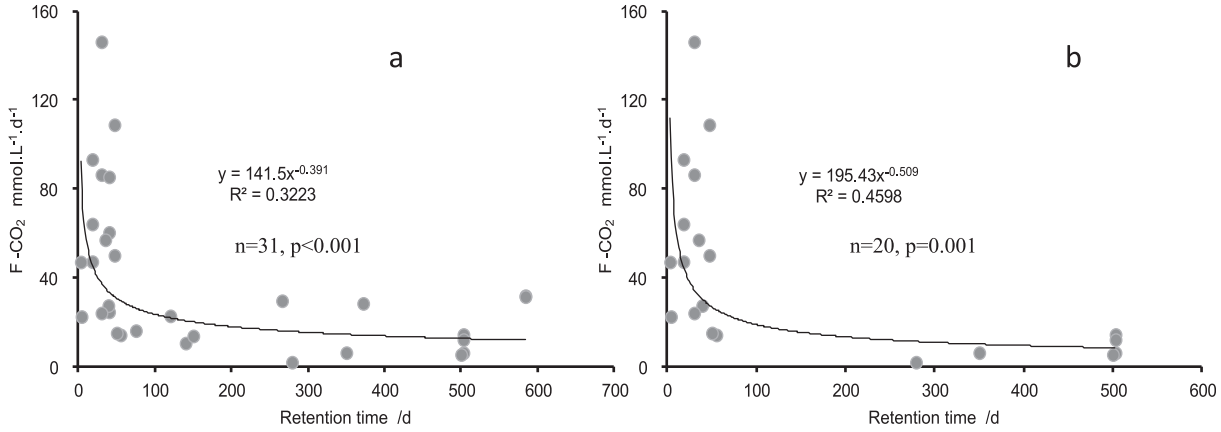

Fig. 7. Scatter plot of hydrological retention time versus average CO_2 emission flux from reservoirs (latitude between 18° and 47°(a) and 20°–30°(b)). Data partly from Barros et al., 2011. Among their data-set, reservoirs in high latitude and tropical area were not included in this plot. This is because, in high latitude reservoir, the long ice cover period in cold season limits CO_2 emission from reservoir surface, which will be emitted rapidly when ice-melting. Consequently, this may bring an underestimation of the annual CO_2 flux if without detailed monitoring in this period. For the same reason, flux with negative value was also not included. Reservoirs in tropical area generally have quite high CO_2 emission, which should be explained by other mechanism. Other data cited from Xiao et al., 2013; Wang et al., 2011; Yu et al., 2008 and this study.

Table 1
Emission flux of CO_2 from the Xinanjiang Reservoir.

	Area[a]/ km^2	Emission/ kton a^{-1}	Invasion/ kton a^{-1}	Net flux/ kton a^{-1}
River reach[b]	40	6.0	−2.4	3.6
Central reservoir[b]	527.4	82.9	−32.7	50.2
Total reservoir surface	567.4	88.9	−35.1	53.8
Downstream[c]	–	52.3	–	52.3
Turbine[c]	–	9.2		9.2
Summation	–	150.4	−35.1	115.3

[a] Data from Zhejiang Administration of Surveying Mapping and Geo-information.
[b] For CO_2 surface flux calculation, the diffusion flux multiplied the area and the days representing by sampling seasons. This calculation didn't take the variation of water surface area into account, due to the water regulation by reservoir. This may bring some uncertainty in the results.
[c] The emission of CO_2 from downstream was calculated as follows: the difference between annual average of pCO_2 in downstream and atmosphere CO_2 (385 μatm) multiplied Kh which was corrected by annual average of water temperature, and then multiplied the annual discharge of the Xinanjiang River (11.26×10^9 m^3 a^{-1}), assuming that all super-saturation CO_2 was released, and pCO_2 in downstream water decreased to atmosphere CO_2 level during its downward transport. The same method used to calculate the turbine emission flux, using the difference between the annual average pCO_2 in downstream and in water 30 m in depth of reservoir.

5. Conclusions

Based on the investigation on a large reservoir (Xinanjiang) in subtropical area, this study found that CO_2 diffusion from the reservoir surface had important seasonal patterns. According to our estimates, about 88.86 kton a^{-1} CO_2 was emitted to the atmosphere in cold seasons from the reservoir surface, while 39% of this flux was re-absorbed back into the reservoir in warm seasons. However, downstream of the dam had quite high CO_2 degassing flux, which is comparable to the net flux from the reservoir surface. In comparison with reservoirs in other area, the Xinanjiang Reservoir in the present study had lower CO_2 flux, which is obviously lower than that of tropical reservoirs, and is at the similar level of boreal reservoirs.

Consequently, we argue that the seasonal patterns of CO_2 diffusion flux from reservoir surface and the quite high CO_2 flux in the downstream should be paid more attention, when estimating the CO_2 emission from the global reservoirs, especially the hydroelectrical reservoir.

Acknowledgments

We are grateful to two anonymous reviewers for their valuable comments and suggestions on this manuscript. We also thank Miss Zhao from NYU for her careful revision in English. This study is funded by the National Natural Science Foundation of China (No. 41273128), the Special S&T Project on Treatment and Control of Water Pollution (No. 2012ZX07104-001), and the Shanghai Education Committee Fund (No. 12YZ017).

Appendix A. Supplementary data

Supplementary data related to this article can be found at http://dx.doi.org/10.1016/j.atmosenv.2014.12.042.

References

Abril, G., Etcheber, H., Borges, A.V., Frankignoulle, M., 2000. Excess atmospheric carbon dioxide transported by rivers into the Scheldt estuary. Earth Planet. Sci. 330, 761–768.
Abril, G., Guérin, F., Richard, S., Delmas, R., Galy-Lacaux, C., et al., 2005. Carbon dioxide and methane emissions and the carbon budget of a 10-year old tropical reservoir (Petit Saut, French Guiana). Glob. Biogeochem. Cycles 19. http://dx.doi.org/10.1029/2005GB002457.
Aucour, A.M., Sheppard, S.M.F., Guyomar, O., Wattelet, J., 1999. Use of 13C to trace origin and cycling of inorganic carbon in the Rhône River system. Chem. Geol. 159, 87–105.
Barros, N., Cole, J.J., Tranvik, L.J., Prairie, Y.T., Bastviken, D., Huszar, V.L., del Giorgio, P., Roland, F., 2011. Carbon emission from hydroelectric reservoirs linked to reservoir age and latitude. Nat. Geosci. 4, 593–596.
Barth, J.A.C., Cronin, A.A., Dunlop, J., Kalin, R.M., 2003. Influence of carbonates on the riverine carbon cycle in an anthropogenically dominated catchment basin: evidence from major elements and stable carbon isotopes in the Lagan River (N. Ireland). Chem. Geol. 200, 203–216.
Borges, A.V., Morana, C., Bouillon, S., Servais, P., Descy, J.-P., Darchambeau, F., 2014. Carbon cycling of Lake Kivu (East Africa): net autotrophy in the epilimnion and emission of CO_2 to the atmosphere sustained by geogenic inputs. PLoS ONE 9 (10), e109500. http://dx.doi.org/10.1371/journal.pone.0109500.
Chamberland, A., Levesque, S., 1996. Hydroelectricity, an option to reduce greenhouse gas emissions from thermal power plants. Energy Convers. Manag. 37 (6–8), 885–890.
Cole, J.J., Caraco, N.F., 1998. Atmospheric exchange of carbon dioxide in a low-wind oligotrophic lake measured by the addition of SF6. Limnol. Oceanogr. 43 (4), 647–656.
Cole, J.J., Caraco, N.F., 2001. Carbon in catchments: connecting terrestrial carbon losses with aquatic metabolism. Mar. Freshw. Res. 52, 101–110.
Copin-Montegut, C., 1985. A method for the continuous determination of the partial pressure of carbon dioxide in the upper ocean. Mar. Chem. 17, 13–21.
Demarty, M., Bastien, J., Tremblay, A., Hesslein, R.H., Gill, R., 2009. Greenhouse gas emissions from boreal reservoirs in Manitoba and Québec, Canada, measured with automated systems. Environ. Sci. Technol. 43, 8908–8915.

Dos Santos, M.A., Rosa, L.P., Sikar, B., Sikar, E., Santos, E.O.d., 2006. Gross greenhouse gas fluxes from hydro-power reservoir compared to thermo-power plants. Energy Policy 34 (4), 481–488.
Duchemin, E., Lucotte, M., Canuel, R., Chamberland, A., 1995. Production of the greenhouse gases CH_4 and CO_2 by hydroelectric reservoirs of the boreal region. Glob. Biogeochem. Cycles 9 (4), 529–540.
Fearnside, P.M., 2002. Greenhouse gas emissions from a hydroelectric reservoir (Brazil's Tucuruí Dam) and the energy policy implications. Water Air Soil Pollut. 133 (1–4), 69–96.
Frankignoulle, M., Borges, A., Biondo, R., 2001. A new design of equilibrator to monitor carbon dioxide in highly dynamic and turbid environments. Water Res. 35 (5), 1344–1347.
Giles, J., 2006. Methane quashes green credentials of hydropower. Nature 444 (30), 524–525.
Hélie, J.F., Hillaire-Marcel, C., Rondeau, B., 2002. Seasonal changes in the sources and fluxes of dissolved inorganic carbon through the St. Lawrence River – isotopic and chemical constraint. Chem. Geol. 186, 117–138.
Humborg, C., Blomqvist, S., Avsan, E., Bergensund, Y., Smedberg, E., 2002. Hydrological alterations with river damming in northern Sweden: implications for weathering and river biogeochemistry. Glob. Biogeochem. Cycles 16 (3), 1–13.
Huttunen, J.T., Visnen, T.S., Hellsten, S.K., et al., 2002. Fluxes of CH_4, CO_2, and N_2O in hydroelectric reservoirs Lokka and Porttipahta in the northern boreal zone in Finland. Glob. Biogeochem. Cycles 16, 1–17.
Jarvic, H.P., Neal, C., Leach, D.V., Robson, A.J., 1997. Major ion concentrations and the inorganic carbon chemistry of the Humber Rivers. Sci. Total Environ. 194-195, 285–302.
Kelly, C.A., Rudd, J.W.M., Bodaly, R.A., et al., 1997. Increases in fluxes of greenhouse gases and methyl mercury following flooding of an experimental reservoir. Environ. Sci. Technol. 31, 1334–1344.
Raymond, P.A., Caraco, N.F., Cole, J.J., 1997. Carbon dioxide concentration and atmospheric flux in the Hudson River. Estuaries 20 (2), 381–390.
Raymond, P.A., Hartmann, J., Lauerwald, R., et al., 2013. Global carbon dioxide emissions from inland waters. Nature 503, 355–359.
Richey, J.E., Melack, J.M., Aufdenkampe, A.K., Ballester, V.M., Hess, L.L., 2002. Outgassing from Amazonian Rivers and wetlands as a large tropical source of atmospheric CO_2. Nature 416, 617–620.
Richey, J.E., 2003. Pathways of atmospheric CO_2 through fluvial systems. In: Field, C.B., Raupach, M. (Eds.), Scientific Committee on Problems of the Environment (SCOPE) United Nations Environment Programme (UNEP)-The Global Carbon Cycle: Integrating Humans, Climate, and the Natural World, vol. 62. Island Press, USA, pp. 329–340.
Roland, F., Vidal, L.O., Pacheco, F.S., et al., 2010. Variability of carbon dioxide flux from tropical (Cerrado) hydroelectric reservoirs. Aquat. Sci. 72, 283–293.
St Louis, V.L., Kelly, C.A., Duchemin, E., Rudd, J.M.V., et al., 2000. Reservoir surfaces as sources of greenhouse gases to the atmosphere: a global estimate. BioScience 50 (9), 766–775.
Teodoru, C.R., Bastien, J., Bonneville, M., et al., 2012. The net carbon footprint of a newly created boreal hydroelectric reservoir. Glob. Biogeochem. Cycles 26, GB2016. http://dx.doi.org/10.1029/2011GB004187.
Teodoru, C.R., Prairie, Y., del Giorgio, P., 2011. Spatial heterogeneity of surface CO_2 fluxes in a newly created Eastmain-1 reservoir in Northern Quebec, Canada. Ecosystems 14, 28–46.
Tremblay, A., Varfalvy, L., Roehm, C., Garneau, M., 2005. Greenhouse Gas Emissions—fluxes and Process: Hydroelectric Reservoirs and Natural Environments. Springer, New York.
Victor, D.G., 1998. Strategies for cutting carbon. Nature 395, 837–838.
Wang, F.S., Wang, B.L., Liu, C.Q., Wang, Y.C., Guan, J., Liu, X., Yu, Y., 2011. Carbon dioxide emission from surface water in cascade reservoirs–river system on the Maotiao River, southwest of China. Atmos. Environ. 45, 3827–3834.
Xiao, S.B., Wang, Y.C., Liu, D.F., et al., 2013. Diel and seasonal variation of methane and carbon dioxide fluxes at Site Guojiaba, the Three Gorges Reservoir. J. Environ. Sci. 25 (10), 2065–2071.
Yang, C., Telmer, K., Veizer, J., 1996. Chemical dynamics of the "St. Lawrence" riverine system: δDH_2O, $\delta 18OH_2O$, $\delta 13CDIC$, $\delta 34S$ sulfate, and dissolved 87Sr/86Sr. Geochim. Cosmochim. Acta 60, 851–866.
Yao, G., Gao, Q., Wang, Z., Huang, X., He, T., Zhang, Y., Jiao, S., Ding, J., 2007. Dynamics of CO_2 partial pressure and CO_2 outgassing in the lower reaches of the Xijiang River, a subtropical monsoon river in China. Sci. Total Environ. 376, 255–266.
Yu, Y., Liu, C.-Q., Wang, F., et al., 2008. Spatiotemporal characteristics and diffusion flux of partial pressure of dissolved carbon dioxide (pCO_2) in Hongjiadu reservoir. Chin. J. Ecol. 27 (7), 1193–1199 (in Chinese, with English abstract).